Research Article

INTERNATIONAL JOURNAL OF CURRENT MEDICAL AND PHARMACEUTICAL RESEARCH

ISSN: 2395-6429, Impact Factor: 4.656
Available Online at www.journalcmpr.com
Volume 5; Issue 08(A); August 2019; Page No. 4481-4488
DOI: http://dx.doi.org/10.24327/23956429.ijcmpr201908726

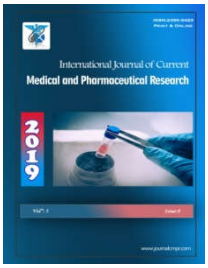

PTEN/YAP MEDIATED LIPID ACCUMULATION IN PODOCYTES CONTRIBUTES TO GLOMERULOSCLEROSIS

Huizhen Wang M. D[1,2], Yangyang Zuo M. D[1, 2], Jianteng Xie M. D[1], Sheng Li M. D[1], Jing Li M.D[1], Tiantian Liang M.D[1], Menglei Jv M. D[1], Yifan Zhang M.D[1], Yanhui Wang M.D[1], Feng Wen M. D[1], Zhiming Ye M. D[1], Shuangxin Liu M. D[1], Xinling Liang M. D[1], Aiqing Li M. D[2], Xueqing Yu M. D[1] and Wenjian Wang Ph.D[1*]

[1]Division of Nephrology, Guangdong Provincial People's Hospital, Guangdong Academy of Medical Sciences, Guangzhou, 510080, China
[2]State Key Laboratory of Organ Failure Research, National Clinical Research Center of Kidney Disease, Division of Nephrology, Nanfang Hospital, Southern Medical University, Guangzhou, 510515, China
Huizhen Wang, Yangyang Zuo, and Jianteng Xie contributed equally to this work.

ARTICLE INFO

Article History:
Received 06th May, 2019
Received in revised form 14th June, 2019
Accepted 23rd July, 2019
Published online 28th August, 2019

Key words:

Foam cell; glomerulosclerosis; high fat diet; phosphatase and tensin homolog deleted on chromosome ten; podocyte; yes-associated protein

ABSTRACT

Objectives: Lipid deposition in glomeruli is one of the pathological characteristics of focal segmental glomerulosclerosis (FSGS). We have showed that phosphatase and tensin homolog (PTEN) is down-regulated in podocytes from patients with FSGS. However, the role of PTEN in FSGS is still largely unknown.

Methods:PTEN partial knockout mouse was used to establish a glomerulosclerosis mouse model induced by uninephrectomy and high fat diet. Oxidized low-density lipoprotein (ox-LDL) stimulated mouse podocyte (cell line) was used to explore the pathway involved in PTEN mediated lipid accumulation.

Results: We revealed that PTEN was down-regulated in lipid accumulated podocytes in human FSGS by immunohistochemistry. Partial deletion of PTEN increased lipid accumulation and fibrotic proteins deposition in glomeruli segmentally, and boosted albuminuria in glomerulosclerosis mouse model. The lipid retention regulated by PTEN in ox-LDL treated podocytes was mainly attributed to SR-A mediated lipid influx rather than lipid synthesis and effusion. Mechanistically, we identified that PTEN regulated yes-associated protein (YAP) activity and subcellular localization independent of Hippo pathway, and PTEN directly bound and dephosphorylating YAP at Ser^{127} in cytoplasm of ox-LDL treated podocytes.

Conclusion: These findings implicate a central role of PTEN in a signaling cascade mediating lipid-loading in podocytes which contributes to glomerulosclerosis, and provide evidence for PTEN/YAP as a target for FSGS therapy.

INTRODUCTION

Accumulation of lipid in glomeruli is one of the pathological characteristicsof focal segmental glomerulosclerosis (FSGS) and associated with the progression of chronic kidney disease (CKD).(1) Although foam cell has been sufficiently elucidated as the key precursor in atherosclerosis, little is known in kidney. It is well accepted that subendothelial macrophages recruited by lipid accumulation engulfs oxidized low-density lipoprotein (ox-LDL) via scavenger receptors (SRs), transforms into foam cells, and causes atherosclerosis.(2-4) Extrapolating from atherosclerosis, foam cells in FSGS have been traditionally regarded as being derived from macrophages, whereas recent studies have indicated that lipid was also taken up by renal cells.(5-10) Emerging studies demonstrated new perspectives into the role of lipid biology as key determinant of podocyte function and survival in kidney diseases such as diabetic kidney disease (DKD) and FSGS.(11-13) It is worthy of note that podocyte expresses SRs, and molecules involved in cellular cholesterol homeostasis including ABCA1, APOL1, and SREBP, holding great promise to convert into foam cell.(11, 14-18) Nevertheless, the underlying mechanism of lipid metabolism disorder in podocytes in glomerulosclerosis needs further study.

Corresponding author:* **Wenjian Wang Ph.D
Division of Nephrology, Guangdong Provincial People's Hospital, Guangdong Academy of Medical Sciences, Guangzhou, 510080, China

Phosphatase and tensin homolog deleted on chromosome ten (PTEN) is a vital tumor suppressor involved in cell proliferation, survival, and motility.(19, 20) PTEN played a critical role in podocyte injury.(21-23) In our and other published studies in diabetic mice, loss of PTEN in podocytes predisposes to the development of proteinuria and glomerulosclerosis, whereas overexpression of PTEN reduces the renal cholesterol retention and slows down the progression of glomerular sclerosis.(24, 25)Indeed, we previously detecte that PTEN is significantly down-regulated in podocytes from patients with FSGS by immunofluorescence.(25)However, whether PTEN plays a role in lipid accumulation in podocytes and contributes to glomerulosclerosis has never been illustrated yet.

In current study, we firstly investigated the expression pattern of PTEN in podocytes with foamy appearance from patients with biopsy-proven FSGS. Then, we generated PTEN partial knockout mouse to confirm the role of PTEN in glomerulosclerosis mouse model. Further, we explored the pathway involved in PTEN mediated lipid accumulation in cultured podocytes subjected to ox-LDL.

MATERIAL AND METHODS

Human study

Human kidney biopsy specimens were obtained from extra reserved tissue of patients with biopsy-proven FSGS. Normal kidney tissues (6 cases) divided to neoplastic lesions were pathologically confirmed and served as normal group. All human studies were performed with the approval of the Ethics Committee of Guangdong Provincial People's Hospital, and written informed consent was obtained from the patients.

Transgenic mouse and glomerulosclerosis mouse model

$PTEN^{+/-}$ mice were established as previously described.(26) Uninephrectomy and diet intervention were employed to establish glomerulosclerosis mice model. Rodent diet with 60 kcal% fat (D12492) was used as high fat diet (HFD) while rodent diet with 10 kcal% fat (D12450B, Research Diets, Inc.) as normal diet (ND). About 20 g-weight, 8-week-old $PTEN^{+/+}$ and $PTEN^{+/-}$ mice were underwent uninephrectomy, and then randomized into four groups (n=6 in each group): $PTEN^{+/+}$ ND, $PTEN^{+/-}$ ND, $PTEN^{+/+}$ HFD, and $PTEN^{+/-}$ HFD. All animal studies were carried out with the approval of the animal care and use committee of Guangdong Provincial People's Hospital. Mice were housed in a specific pathogen-free environment in a 12 h light/dark cycle. Following 24 weeks of diet intervention, blood and kidney from all mice were collected for further analyses.

Biochemical analysis

The levels of urinary albumin (Mouse Albumin ELISA Kit, Bethyl Laboratories), urine creatinine (Creatinine Urinary Colorimetric Assay Kit) (Cayman Chemicals) were determined according to the manufacturer's protocols.

Periodic acid-silver metheramine (PASM) and Periodic acid-Schiff (PAS) staining

With PAS–stained sections, mesangial matrix areas were quantified in 10 randomly light microscopic views (×400) per mouse in a blinded fashion using an image analysis system (NIS Elements, Nikon, Sendai, Japan). Mesangial matrix index (MMI) was calculated as the ratio of mesangial matrix area to glomerular area ×100 (% area).

Oil Red O staining

Frozen sections were stained with Oil Red O for lipid detection and quantified as described.(25, 27) Briefly, Oil Red O–positive cells were counted in at least 20 high-power (×400) fields with a micro square scale plate (0.0625 mm^2) arranged in ocular lens by two independent researchers in a blinded fashion. The number of Oil Red O–positive cells in glomeruli was represented as cells/mm^2/glomeruli.

Cell culture and treatment

Conditionally immortalized mouse podocytes were cultured as described.(28)Briefly, the podocytes were cultured in RPMI 1640 (Corning, USA) containing 10% fetal bovine serum (FBS) and mouse recombinant interferon gamma (IFN-γ, 50 U/ml, PROSPEC, Israel) at 33°C for proliferation. Subsequently, podocytes were maintained in DMEM containing 5% FBS on BD BioCoat Collagen I plates (BD Biosciences) at 37°C for 8 to 12 days to induce differentiation. PTEN and YAP small interfering RNA (siRNA, RiboBio, China) were transfected into mature podocytes using Lipofectamine 2000TM (Invitrogen) at a final concentration of 50 nmol/L, whereas pDC316-mCMV-EGFP-PTEN (ad-PTEN, Biowit Technologies, China) directly infected podocytes at $1.0X10^{10}$Tu/mL. Bpv (HOpic), an inhibitor of phosphatase activity of PTEN, was added at 1 μmol/L 1 h prior to ox-LDL (Yiyuan Biotechnologies, China).

Immunohistochemistry and immunoblot analysis

Immunohistochemistry and immunoblot were performed according to our previous studies.(25, 27) Collagen I stained was quantified in light microscopic views of 10 consecutive glomerular cross-sections per mouse using an image analysis system (NIS Elements, Nikon, Sendai, Japan). Collagen I stained area was calculated as the ratio of collagen I positive stained area in glomeruli to glomerular area ×100 (% of glomeruli). The following primary antibodies were used: anti-collagen I (Col I, ab34710), anti-PTEN (ab32199), anti-nephrin (ab136894) (Abcam, Cambridge, MA), anti-synaptopodin (sc-515842)(Santa Cruz, Inc), anti-YAP (#14074), anti-Phospho-YAP (Ser^{127}, #13008), anti-Mst1/2 (#3682/#3952), anti-Phospho-Mst ($Thr^{180/183}$, #3681), anti-Lats1/2 (#3477/#5888), anti-Phospho-Lats (Thr^{1079}, #8654), anti-Histone H3 (#4499) (Cell Signaling Technology, USA), and anti-GAPDH (Sigma, Japan).

Immunofluorescence analysis

Concisely, frozen slides were incubated with primary antibodies in 1:100 dilution including anti-PTEN, anti-nephrin, anti-YAP, and anti-synaptopodin followed by corresponding Alexa Fluor secondary antibodies (1:200 dilution, Life Technologies) and DAPI counterstain. The results of immunofluorescence were shot and quantified using a confocal microscope (LSM710, Zeiss).

PCR

Cell total RNA was extracted with Trizol according to the manufacturer's protocol. 1 μg RNA was reverse transcribed using MMLV-RT and random primers at 37℃ for 15 min in a total reaction volume of 20 μL. The PCR amplification was carried out with an initial 4 min denaturation at 94°C, followed by 30 cycles of reaction (94°C, 30 s; 57°C, 30 s; 72°C, 1 min), and a final extension of 72°C for 10 min. The expression

levels of target mRNA were analyzed using $2^{-\Delta\Delta Ct}$ method normalized to internal control of GAPDH mRNA.

Quantification of ABCA1 concentration and HMG-CoA reductase activity

The activity of HMG-CoA reductase was measured basing on the consumption of NADPH by the enzyme, which can be measured by the decrease of absorbance at OD=340 nm using the HMG-CoA Reductase Activity Assay Kit (Colorimetric) (ab204701, Abcam, Cambridge, MA) in accordance with manufacturer's directions. To determine the concentration of ABCA1, Mouse ATP-binding cassette sub-family A member 1(ABCA1) ELISA kit (CSB-EL001033MO, CUSABIO, CN) was performed following the principle of double antibody sandwich method.

Proximity ligation assay (PLA)

PLA was performed according to the protocol of Duolink® PLA Fluorescence (sigma-aldrich). Podocytes on coverslips were fixed and permeabilized in preparation. Firstly, coverslips were incubated with blocking solution for 60 min at 37°C. Then, coverslips were incubated with primary antibodies overnight at 4℃, anti-PTEN (ab79156) and anti-Phospho-YAP (Ser^{127}). After wash, PLA probes and ligation were incubated with podocytes for 60 min and 30 min at 37°C, respectively. For amplification, polymerase was applied to coverslips for 100 min at 37°C. Finally, coverslips were mounted with Duolink In Situ Mounting Medium with DAPI, and analyzed in a confocal microscope.

Co-immunoprecipitation (CoIP)

Podocytes were lysed in lysis buffer (Piece) with protease and phosphatase inhibitors. The cell lysate was blocked with Dynabeads™ Protein G (Thermo Fisher Scientific) for 1 h at 4°C. Adsorbed by DynaMag™-Spin Magnet (Thermo Fisher Scientific), the supernatants were then incubated with anti-YAP at a final concentration of 1 μg overnight at 4°C, and subsequently Protein G for 2 h. Finally, YAP-interacting proteins were eluted from beads by lysing in 2× SDS-sample buffer for 15 min on ice and heating for 10 min at 50°C prior to denaturation. The samples were analyzed by western blotting with anti-PTEN and anti-Lats1. The same amount of normal rabbit IgG-AC (sc-2345, Santa Cruz) was used as control.

Glutathione-S-transferse (GST) pulldown assay

Plasmid pGEX-4T-1-GST-PTEN was expressed in Escherichia coli BL21 as a GST-fusion protein, GST-vector as negative control. Briefly, individual E. coli BL21 colony was transferred to lysogeny broth (LB) and shaken overnight at 37 °C. Thirty-fold diluted in 30 ml LB and incubated for 2~3 h at 37 °C until the OD600 reached 0.6. Isopropyl-β-d-thiogalactoside was added at 0.1 mM to induce GST-fusion proteins expression for 3 h at 20 °C. Then, GST-vector or GST-PTEN fusion proteins were purified, immobilized on GST beads (GE Healthcare), incubated with purified p-YAP (Ser^{127}) protein extracted from ox-LDL stimulated podocytes overnight at 4 °C, and eluted by glutathione, sequentially. Pull down complexes were analyzed by western blotting with anti-Phospho-YAP (Ser^{127}).

Statistical analysis

All data are presented as mean ± SD. *One-way ANOVA* followed by *Bonferroni* multiple-comparison test was performed to compare parametric values among three or more groups. An independent samples *t*-test was performed for comparison between two groups using Graph-Pad Prism 5.0 (Graph Pad Software, San Diego, CA). A P value <0.05 was considered statistically significant.

RESULTS

1. PTEN was down-regulated in lipid accumulated podocytes in human FSGS

By immunohistochemistry, foamy appearance was detected in podocytes in FSGS as indicated by synaptopodin, a marker of podocyte, and PTEN was found to be markedly reduced in foamy podocytes and sclerotic areas of FSGS compared with normal glomeruli (Figure 1).

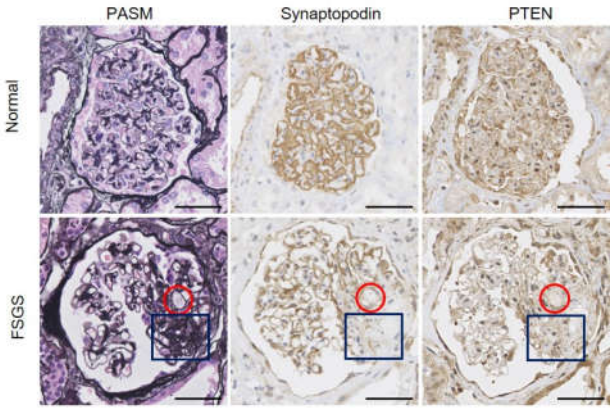

Figure 1 Expression of PTEN in human glomeruli of FSGS

Representative periodic acid-silver metheramine (PASM) staining (left column), immunohistochemical staining of synaptopodin (middle column) and PTEN (right column) in glomeruli from normal kidney samples and patients with biopsy-proven FSGS. Foamy podocyte as indicated by synaptopodin was marked in red round. Sclerosis area was marked in blue square. Scale bar, 50 μm.

2. Partial deficiency of PTEN aggravated glomerular lipid accumulation and glomerulosclerosis

Consistently, immunofluorescence revealed that PTEN was also significantly decreased in podocytes from uninephrectomized mice consuming HFD compared with ND (Figure 2, A and B).

To investigate the contribution of PTEN to glomerulosclerosis *in vivo*, partial knockout of PTEN ($PTEN^{+/-}$) mice were generated, and identified by PCR and western blotting ($PTEN^{+/+}$ mice were served as control)(Figure 2, C and D). Uninephrectomized mice consuming HFD developed progressive albuminuria compared with ND as measured by urinary albumin/creatinine ratio (ACR). However, urinary albumin excretion was higher at 16 weeks, and significantly increased at 24 weeks of age in $PTEN^{+/-}$ mice relative to $PTEN^{+/+}$ mice (Figure 2E). Uninephrectomy and HFD also caused glomerular fibrosis and sclerosis in manifestation of mesangial matrix expansion and collagen I accumulation. Exposure to HFD, PTEN deficiency substantially accentuated the progression of glomerulosclerosis (Figure 2, F-I). In addition, the number of foam cells as indicated by Oil red positive cells per glomerulus was markedly increased in uninephrectomized mice fed with HFD compared with ND. Surprisingly, knockout of PTEN aggravated the lipid retention in glomeruli under HFD (Figure 2, J and K).

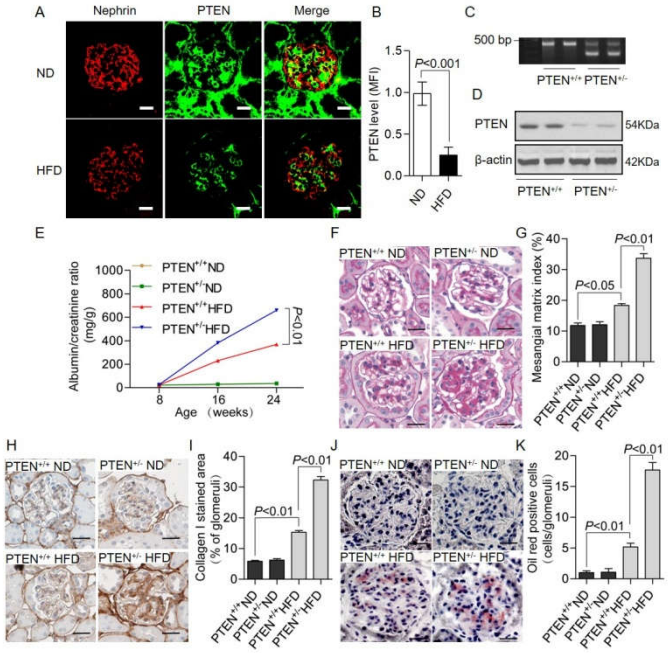

Figure 2 Partial knockout of PTEN aggravated glomerular lipid accumulation and glomerulosclerosis in mice

(A) Representative immunofluorescence labeling of PTEN in glomeruli from uninephrectomized mice fed with ND and HFD. Nephrin, red; PTEN, green; Merge, yellow. Scale bar, 20 μm. (B) Quantification of mean fluorescence intensity (MFI) of PTEN in glomeruli area. N = 10 glomeruli per group, statistic was calculated by *t*-test.(C) Identification of partial knockout of *Pten* gene in kidney by PCR.(D) Identification of partial knockout of *Pten* gene in kidney by western blotting. (E) Urinary albumin/creatinine ratio (ACR) was calculated at indicated time points from 4 groups of mice: uninephrectomized $PTEN^{+/+}$ ND, $PTEN^{+/-}$ ND, $PTEN^{+/+}$ HFD and $PTEN^{+/-}$ HFD mice.(F) Representative PAS staining of glomeruli from 4 groups of mice. Scale bar, 25 μm. (G) Quantification of mesangial matrix expansion by mesangial matrix index (MMI).(H) Representative immunohistochemical staining of collagen I in glomeruli from 4 groups of mice. Scale bar, 25 μm.(I) Quantification of collagen I stained area per glomeruli area (%).(J) Representative Oil Red O staining of glomeruli from 4 groups of mice. Scale bar, 20 μm.(K) Quantification of Oil Red O-positive cell number per mm^2.Statistics of 4 groups of mice (n=6 mice per group) were calculated by *One-way ANOVA* and *Bonferroni* multiple-comparison test. ND, normal diet; HFD, high-fat diet.

3. PTEN regulated lipid loading via SR-A mediated lipid influx in podocytes

To mimic foamy podocytes *in vitro*, cultured mouse podocytes were treated with ox-LDL. We examined the molecules related to lipid metabolism by q-RCR and found that the expression of SRs including SR-A, CD36, and LDLr was changed exposed to ox-LDL in podocytes. However, unlike CD36 and LDLr, SR-A was discovered to be significantly regulated by PTEN. Inhibition of PTEN either in abundance or phosphatase activity aggravated the up-regulation of SR-A in ox-LDL stimulated podocytes, whereas enhancement of PTEN interdicted the effect of ox-LDL on SR-A (Figure 3, A-D). In addition, we found that PTEN had no significant effect on molecules related to lipid effusion or synthesis in ox-LDL treated podocytes, particularly the concentration of ABCA1 and activity of HMG-CoA reductase (Figure 3, E-I).

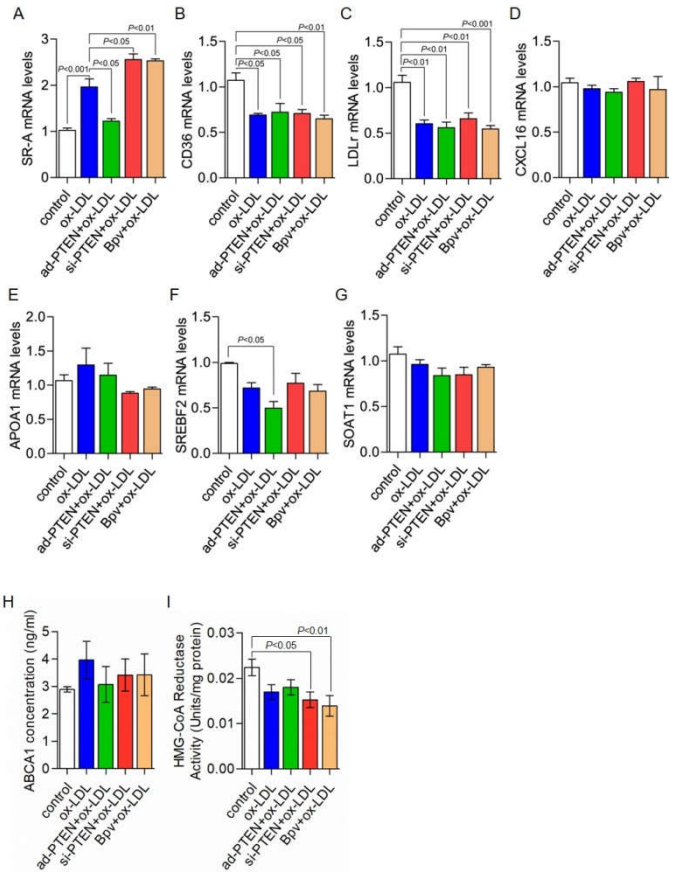

Figure 3PTEN regulated SR-A mediated lipid influx in ox-LDL stimulated podocytes

(A-G) Quantification of SR-A, CD36, LDLr, CXCL 16, APOA1, SREBF2, and SOAT1 mRNA levels in podocytes treated with 20 μg/ml ox-LDL. SR-A, scavenger receptor A; CD36, cluster of differentiation 36; LDLr, low-density lipoprotein receptor; CXCL 16, chemokine ligand 16; APOA1, apolipoprotein A-I; SREBF2, sterol regulatory element binding transcription factor 2; SOAT1, sterol-O-acyltransferase 1.(H) Quantification of ATP-binding cassette transporter 1 (ABCA1) concentration in podocytes.(I) Quantification of 3-hydroxy-3-methyl-glutaryl coenzyme A (HMG-CoA) reductase activity in podocytes (normalized by protein concentration).Statistics among groups were calculated by *One-way ANOVA* and *Bonferroni* multiple-comparison test.

4. PTEN regulated YAP activity and subcellular localization independent of Hippo pathway

By western blotting, we detected that ox-LDL caused a significant reduction in nuclear YAP and a marked increase in the level of p-YAP (Ser^{127}) in podocytes, whereas ox-LDL had no effect on the abundance or phosphorylation of the upstream of Hippo-YAP pathway including Mst1/2 and Lats1/2(Figure 4). Further, we revealed that forced PTEN restrained the elevation of p-YAP (Ser^{127}) in podocytes challenged with ox-LDL. Conversely, silencing PTEN or inhibiting phosphatase activity of PTEN by Bpv significantly aggravated the elevation of p-YAP(Ser^{127}). Simultaneously, exposure to ox-LDL, PTEN led to no alteration in either abundance or phosphorylation of the upstream of Hippo-YAP pathway (Figure 5A). By confocal microscopy, YAP dominantly distributed in podocyte nucleus under normal conditions. Exposure to ox-LDL YAP was transferred from nucleus into cytoplasm in podocytes. Indeed, enhanced PTEN restrained YAP from transfering into cytoplasm, resulting a robust increase in nuclear YAP, whereas inhibition of PTEN exhibited opposite effect. In addition, we found that ox-LDL slightly destroyed cytoskeleton indicated by synaptopodin in podocytes. Either knockdown or enzymatic activity inhibition of PTEN aggravated cytoskeleton destruction in ox-LDL treated podocytes, whereas

overexpression of PTEN exhibited protective effect(Figure 5B).

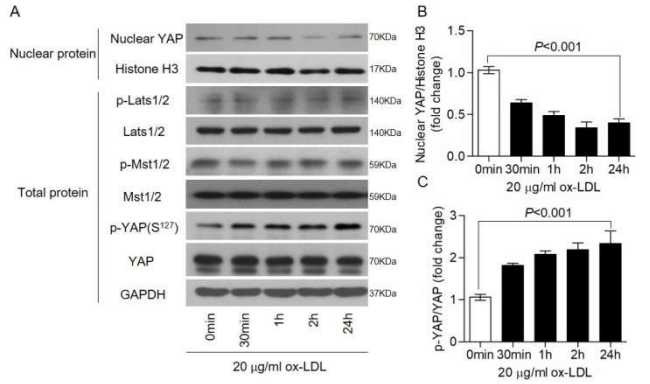

Figure 4 Ox-LDL affected the activation and translocation of YAP independent of Hippo pathway

(A) Representative western blotting of Hippo signal pathway in ox-LDL stimulated podocytes at indicated times.(B) Densitometric analyses of nuclear YAP protein expression in ox-LDL stimulated podocytes.(C) Densitometric analyses of p-YAP (Ser^{127}) levels in ox-LDL stimulated podocytes.Statistics of western blotting were from three independent experiments. Statistics among groups were calculated by *One-way ANOVA*. *Bonferroni* multiple-comparison test was performed between group 0 min and 24 h.

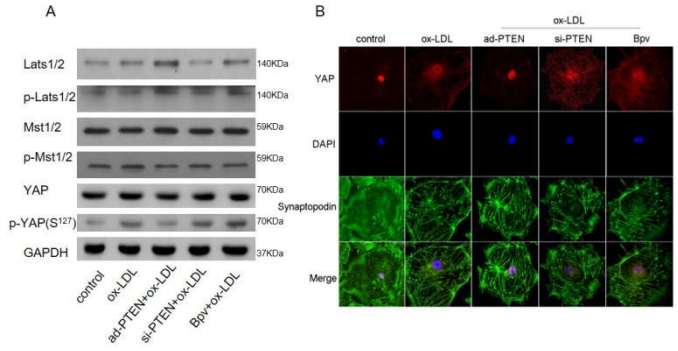

Figure 5PTEN regulated the activation and translocation of YAP independent of Hippo pathway in ox-LDL stimulated podocytes

(A) Representative western blotting of Hippo signal pathway in ox-LDL stimulated podocytes exposed to ad-PTEN, si-PTEN, and Bpv, respectively.(B) Representative immunofluorescence labeling of YAP in ox-LDL stimulated podocytes exposed to ad-PTEN, si-PTEN, and Bpv, respectively. Cell nucleus, blue; Synaptopodin, green; YAP, red. Scale bar, 10 μm.

5. PTEN directly bound with p-YAP (Ser^{127})

Firstly, we performed an endogenous co-immunoprecipitation using YAP antibody as the bait and detected a compound containing PTEN and YAP without kinase Lats1 (Figure 6A). PLA using a mix of anti-PTEN and p-YAP (Ser^{127}) antibodies showed red fluorescence dots in podocytes, whereas nearly no fluorescence detected in either negative control displayed by use of anti-PTEN or p-YAP (Ser^{127}) antibody alone or podocytes depleted for PTEN or YAP. As expected, the endogenous molecular proximity between PTEN and p-YAP (Ser^{127}) was localized in the cytoplasm (Figure 6B). Importantly, using ectogenic recombinant GST-PTEN, we pulled down purified p-YAP (Ser^{127}) protein extracted from ox-LDL stimulated podocytes (Figure 6C).

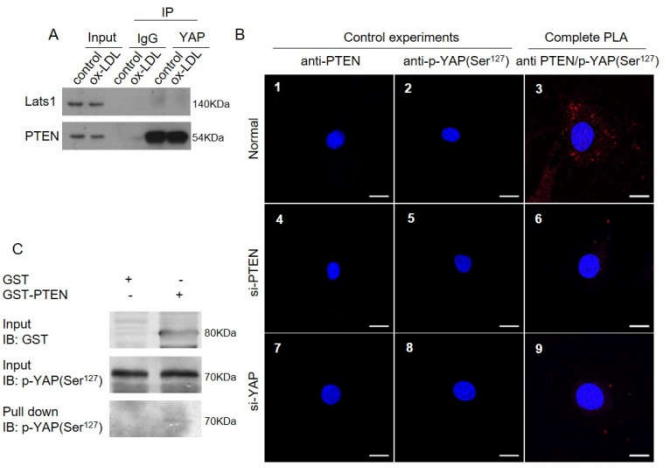

Figure 6 PTEN bound with p-YAP at Ser^{127}

(A) Total lysate of podocytes under control and ox-LDL condition was collected for immunoprecipitation using a YAP antibody as the bait, and analyzed by western blotting using Lats1 and PTEN antibodies.(B) Results of Proximity Ligation Assay (PLA) with PTEN and p-YAP (Ser^{127}) on cultured podocytes. 1-3: PLA on normal podocytes; 1-2: Control experiments with only one of the primary antibodies; 3: Complete PLA with PTEN and p-YAP (Ser^{127}) antibodies. 4-6: PLA after inhibition of PTEN on podocytes; 4-5: Control experiments with only one of the primary antibodies; 6: Complete PLA with PTEN and p-YAP (Ser^{127}) antibodies. 7-9: PLA after inhibition of YAP on podocytes; 7-8: Control experiments with only one of the primary antibodies; 9: Complete PLA with PTEN and p-YAP (Ser^{127}) antibodies. Scale bar, 20 μm.(C) Purified GST-vector or GST-PTEN fusion proteins, immobilized on GST beads, were incubated with purified p-YAP (Ser^{127}) protein extracted from ox-LDL stimulated podocytes. Pull down complexes were analyzed by western blotting using p-YAP (Ser^{127}) antibody.

DISCUSSION

In our study, we provide several novel findings regarding the mechanism of PTEN/YAP pathway on glomerulosclerosis. First, we showthat PTEN/YAP pathway mediates lipid accumulation in podocytes and contributes to the pathogenesis of glomerulosclerosis, which challenges the infiltration of glomerular foam cells derived from macrophage in traditional concept. We verify the expression of PTEN in foamy podocytes of patients with FSGS. Second, with a partial PTEN knockout mouse model, we confirm the protective role of PTEN in foamy podocytes formation and glomerulosclerosis. Third, we describe the underlying mechanism that PTEN directly binds with p-YAP (Ser^{127}) and consequently down-regulates SR-A expression, resulting in suppressing lipid retention in podocytes.

Although foam cells were present in glomeruli of FSGS, and were traditionally determined to be derived from macrophages,(1, 6, 29) few or no CD68^{+} histiocytes were detected in foamy-appearing glomeruli, suggesting that resident glomerular cells might transform into foam cells themselves and cause glomerulosclerosis.(30) It was noteworthy that unbalanced cholesterol and free fatty acids caused excess intracellular lipid accumulation, podocyte injury, and eventually kidney diseases.(12, 31)Herein, we found that PTEN was down regulated in podocytes with plentiful lipid droplets in patients with FSGS. Emerging studies proposed that PTEN played an important role in glomerular injury and fibrosis.(24, 32-34)PTEN/PI3K/AKT and PTEN/Rac1/Cdc42 pathways have a significant effect on controlling glucose tolerant or cytoskeletal rearrangement, playing a vital role in DKD. However, disorder of lipid metabolism rather than high glucose is one of the main pathogenies of glomerulosclerosis in FSGS. Recently, PTEN was discovered to be involved in cell lipid biology.(35,

36)However, whether PTEN causes glomerular diseases via mediating podocyte lipid metabolism remains unknown. In our previous study, we identify that podocyte-specific overexpression of PTEN slows down the progression of glomerulosclerosis in HFD-fed mice.(37) In current study, we further revealed that partial knockout of PTEN *in vivo* increased glomerular lipid droplets accumulation and worsened the renal phenotype of glomerulosclerosis.

To investigate how PTEN regulates lipid metabolism in podocytes, we utilized a cultured foamy podocytes model induced by ox-LDL, a key element on the onset of foam cells.(38, 39)Increased synthesis, influx, or decreased efflux were accepted to be critical causes of cellular cholesterol accumulation and foam transformation in podocyte biology.(12, 13)Over-uptake of lipid is the chief trigger of local renal injury that the Watanabe heritable hyperlipidemic rabbit, characterized by a deficiency in LDL receptors, failed to develop renal lesions.(40)Notably, scavenger receptors were the key transmembrane receptors in the endocytosis of modified LDL, and expressed abundantly in podocytes.(12, 13, 16-18)Different from other lipoprotein receptors, SR-A,a key receptor of endocytosis of ox-LDL, was not regulated by cytoplasmic cholesterol via negative feedback, and thus played an important role in foamy cells formation.(35, 41-43)Our previous study demonstrate that deficiency of SR-A significantly reduces the renal lipid accumulation and slows down the progression of nephropathy independent of lipid control under diet-induced hyperlipidemia.(27)Herein, we detected thatPTEN rescued podocytes from foamy alteration by suppressing SR-A mediated lipid influx rather than cholesterol synthesis and efflux implicated by HMG-CoA reductase and ABCA1, respectively.Though we previous reveal that ox‑LDL increases SR‑A expression, and decreases PTEN expression in cultured podocytes, resulting in intracellular cholesterol accumulation and down-regulation of nephrin. Overexpression of PTEN significantly inhibites the expression level of SR‑A and lipid uptake induced by ox‑LDL.(44)As located in cytoplasm, PTEN fails to regulate the expression of SR-A directly and the underlying pathway needs further elucidation.

YAP, a transcriptional co-activator, was the main downstream target of Hippo signaling pathway involved in cell proliferation and apoptosis.(45, 46) Mechanistically, Mst phosphorylated kinases Lats to have YAP phosphorylated at Ser^{127}. Ser^{127} was the highly conserved residues. Phosphorylation of Ser^{127}restricted YAP localization to the cytoplasm in combination with 14-3-3 protein, and inhibited YAP activity. In our and other studies,(47-49) YAP primarily distributed in nucleus in podocytes and worked as a transcription factor in normal condition. We demonstrated that ox-LDL caused a marked increase in the level of p-YAP (Ser^{127})/total YAP ratio which was inversely related to nuclear YAP without altering the upstream of Hippo pathway, suggesting that YAP was failed to be dephosphorylated in response to ox-LDL independent of Hippo pathway. In addition to Hippo pathway, YAP was controlled by a variety of signals such as PI3K pathway.(46, 50, 51) Unexpectedly, inhibitors of Akt hardly affected the activity and expression of YAP, suggesting that YAP was regulated by the upstream of PI3K/Akt pathway.(51, 52)Given that 1) PTEN, an efficient inhibitor of PI3K, dephosphorylated protein and peptide substrates phosphorylated on serine (S);(20)2) YAP bound to Dendrin through the WW domain (of YAP) to PPXY motif (in Dendrin) in podocytes;(47) 3) Though there is no obvious PPXY motif in PTEN, WWP2 bound to PTEN through the phosphatase-domain (of PTEN), where WWP2 was also a WW domain-containing protein,(53)we temporarily speculated that p-YAP (Ser^{127}) was a potential phosphorylated substrate of PTEN in regulation of SR-A. And it is interesting for us to confirm whether PTEN binds to p-YAP (Ser^{127}) through the WW domain of YAP to phosphatase-domain of PTEN in future experiments. Contradictorily, other studies reported that PI3K/Akt pathway was regulated by YAP.(54-56)YAP was found to decrease PTEN protein expression and consequently increase Akt activity by inducing miR-29 to inhibit PTEN translation.(56)Base on the review of other studies and our results, there probably wasa feedback loop between PTEN and YAP.

Over the past years, YAP has emerged as a crucial factor in kidney disease as an inhibitor of podocyte apoptosis.(47, 48)Knockout of YAP in podocytes led to proteinuria and glomerulosclerosis in mice via podocyte depletion.(48) However, whether PTEN/YAP mediates glomerulosclerosis via podocyte apoptosis is not verified in our study.

CONCLUSION

In this study, we found that PTEN was down-regulated in podocytes with foamy appearance from patients with FSGS. Partial knockout of PTEN *in vivo* increased glomerular lipid droplets accumulation and worsened the progression of glomerulosclerosis. Importantly, we revealed that directly binding of PTEN to p-YAP (Ser^{127}) resulted in p-YAP (Ser^{127}) dephosphorylation, YAP activation, and nuclear translocation, consequently suppressed SR-A expression and lipid retention in ox-LDL treated podocytes. Our findings implicate a central role of PTEN in a signaling cascade that regulates podocyte lipid retention which contributes to glomerulosclerosis, and provide evidence for a novel role for PTEN/YAP pathway as a target for FSGS therapy.

Acknowledgments

We thank Professor Farhad R. Danesh (MD Anderson Cancer Research Center) for kindly providing podocin-iCreER^{T2} mice, and Professor Zhaoyong Hu (Division of Nephrology, Baylor College of Medicine) for kindly providing PTEN partial knockout mice.

Funding Sources

This work was supported by grants from the National Natural Science Foundation Committee of China (Grant Nos. 81470974 & 81270816 to WWJ, and 81770727 to LAQ), and GDUPS (2017).

Declaration of Interests

None.

Author Contributions

WWJ, ZYY, XJT and WHZ constructed and identified the transgenic mice and analyzed the biochemical characteristics of them; JML, LTT and ZYF performed and analyzed the expression of PTEN in human subjects and mice, while LS, LJ, WF and WYH charged for histological execution and evaluation; YZM, LSX, LXL and LAQ analyzed data and drafted figures; LAQ and YXQ provided important advices on data analysis; WWJ designed the study; WHZ and WWJ wrote

the paper; all authors revised the paper and approved the final version.

References

1. Stokes MB, Valeri AM, Markowitz GS, D'Agati VD. Cellular focal segmental glomerulosclerosis: Clinical and pathologic features. Kidney Int. 2006;70(10):1783-92.
2. Li AC, Glass CK. The macrophage foam cell as a target for therapeutic intervention. Nat Med. 2002;8(11):1235-42.
3. Tabas I, Bornfeldt KE. Macrophage Phenotype and Function in Different Stages of Atherosclerosis. Circ Res. 2016;118(4):653-67.
4. Liu Z, Zhu H, Dai X, Wang C, Ding Y, Song P, *et al*. Macrophage Liver Kinase B1 Inhibits Foam Cell Formation and Atherosclerosis. Circ Res. 2017;121(9):1047-57.
5. Diamond JR, Karnovsky MJ. Focal and segmental glomerulosclerosis: analogies to atherosclerosis. Kidney Int. 1988;33(5):917-24.
6. Hara S, Kobayashi N, Sakamoto K, Ueno T, Manabe S, Takashima Y, *et al*. Podocyte injury-driven lipid peroxidation accelerates the infiltration of glomerular foam cells in focal segmental glomerulosclerosis. *Am J Pathol*. 2015;185(8):2118-31.
7. Yuan Y, Zhao L, Chen Y, Moorhead JF, Varghese Z, Powis SH, *et al*. Advanced glycation end products (AGEs) increase human mesangial foam cell formation by increasing Golgi SCAP glycosylation in vitro. *Am J Physiol Renal Physiol*. 2011;301(1):F236-43.
8. Chung JJ, Huber TB, Godel M, Jarad G, Hartleben B, Kwoh C, *et al*. Albumin-associated free fatty acids induce macropinocytosis in podocytes. *J Clin Invest*. 2015;125(6):2307-16.
9. Ruan XZ, Varghese Z, Powis SH, Moorhead JF. Dysregulation of LDL receptor under the influence of inflammatory cytokines: a new pathway for foam cell formation. Kidney Int. 2001;60(5):1716-25.
10. Szeto HH, Liu S, Soong Y, Alam N, Prusky GT, Seshan SV. Protection of mitochondria prevents high-fat diet-induced glomerulopathy and proximal tubular injury. Kidney Int. 2016;90(5):997-1011.
11. Pedigo CE, Ducasa GM, Leclercq F, Sloan A, Mitrofanova A, Hashmi T, *et al*. Local TNF causes NFATc1-dependent cholesterol-mediated podocyte injury. *J Clin Invest*. 2016;126(9):3336-50.
12. Fornoni A, Merscher S, Kopp JB. Lipid biology of the podocyte--new perspectives offer new opportunities. Nat Rev Nephrol. 2014;10(7):379-88.
13. Merscher S, Pedigo CE, Mendez AJ. Metabolism, energetics, and lipid biology in the podocyte - cellular cholesterol-mediated glomerular injury. Front Endocrinol (Lausanne). 2014;5:169.
14. Beckerman P, Bi-Karchin J, Park AS, Qiu C, Dummer PD, Soomro I, *et al*. Transgenic expression of human APOL1 risk variants in podocytes induces kidney disease in mice. Nat Med. 2017;23(4):429-38.
15. Jiang T, Wang XX, Scherzer P, Wilson P, Tallman J, Takahashi H, *et al*. Farnesoid X receptor modulates renal lipid metabolism, fibrosis, and diabetic nephropathy. Diabetes. 2007;56(10):2485-93.
16. Zhang Y, Ma KL, Liu J, Wu Y, Hu ZB, Liu L, *et al*. Dysregulation of low-density lipoprotein receptor contributes to podocyte injuries in diabetic nephropathy. *Am J Physiol Endocrinol Metab*. 2015;308(12):E1140-8.
17. Gutwein P, Abdel-Bakky MS, Schramme A, Doberstein K, Kampfer-Kolb N, Amann K, *et al*. CXCL16 is expressed in podocytes and acts as a scavenger receptor for oxidized low-density lipoprotein. *Am J Pathol*. 2009;174(6):2061-72.
18. Cui W, Maimaitiyiming H, Zhou Q, Norman H, Zhou C, Wang S. Interaction of thrombospondin1 and CD36 contributes to obesity-associated podocytopathy. Biochim Biophys Acta. 2015;1852(7):1323-33.
19. 19.Li J, Yen C, Liaw D, Podsypanina K, Bose S, Wang SI, *et al*. PTEN, a putative protein tyrosine phosphatase gene mutated in human brain, breast, and prostate cancer. Science. 1997;275(5308):1943-7.
20. Worby CA, Dixon JE. Pten. Annu Rev Biochem. 2014;83:641-69.
21. Canaud G, Bienaime F, Viau A, Treins C, Baron W, Nguyen C, *et al*. AKT2 is essential to maintain podocyte viability and function during chronic kidney disease. Nat Med. 2013;19(10):1288-96.
22. Fukuda A, Chowdhury MA, Venkatareddy MP, Wang SQ, Nishizono R, Suzuki T, *et al*. Growth-dependent podocyte failure causes glomerulosclerosis. *J Am Soc Nephrol*. 2012;23(8):1351-63.
23. Welsh GI, Hale LJ, Eremina V, Jeansson M, Maezawa Y, Lennon R, *et al*. Insulin signaling to the glomerular podocyte is critical for normal kidney function. Cell Metab. 2010;12(4):329-40.
24. Lin J, Shi Y, Peng H, Shen X, Thomas S, Wang Y, *et al*. Loss of PTEN promotes podocyte cytoskeletal rearrangement, aggravating diabetic nephropathy. *J Pathol*. 2015;236(1):30-40.
25. Wang H, Feng Z, Xie J, Wen F, Jv M, Liang T, *et al*. Podocyte-Specific Knockin of PTEN Protects Kidney from Hyperglycemia. *Am J Physiol Renal Physiol*. 2018.
26. Hu Z, Wang H, Lee IH, Modi S, Wang X, Du J, *et al*. PTEN inhibition improves muscle regeneration in mice fed a high-fat diet. Diabetes. 2010;59(6):1312-20.
27. Wang W, He B, Shi W, Liang X, Ma J, Shan Z, *et al*. Deletion of scavenger receptor A protects mice from progressive nephropathy independent of lipid control during diet-induced hyperlipidemia. Kidney Int. 2012;81(10):1002-14.
28. Wang W, Wang Y, Long J, Wang J, Haudek SB, Overbeek P, *et al*. Mitochondrial fission triggered by hyperglycemia is mediated by ROCK1 activation in podocytes and endothelial cells. Cell Metab. 2012;15(2):186-200.
29. Eom M, Hudkins KL, Alpers CE. Foam cells and the pathogenesis of kidney disease. Curr Opin Nephrol Hypertens. 2015;24(3):245-51.
30. Kaur A, Sethi S. Histiocytic and Nonhistiocytic Glomerular Lesions: Foam Cells and Their Mimickers. Am J Kidney Dis. 2016;67(2):329-36.
31. Wahl P, Ducasa GM, Fornoni A. Systemic and renal lipids in kidney disease development and progression. Am J Physiol Renal Physiol. 2016;310(6):F433-45.
32. McClelland AD, Herman-Edelstein M, Komers R, Jha JC, Winbanks CE, Hagiwara S, *et al*. miR-21 promotes renal fibrosis in diabetic nephropathy by targeting

PTEN and SMAD7. Clin Sci (Lond). 2015;129(12):1237-49.
33. 33.Bhatt K, Wei Q, Pabla N, Dong G, Mi QS, Liang M, *et al*. MicroRNA-687 Induced by Hypoxia-Inducible Factor-1 Targets Phosphatase and Tensin Homolog in Renal Ischemia-Reperfusion Injury. *J Am Soc Nephrol*. 2015;26(7):1588-96.
34. 34.Li Y, Hu Q, Li C, Liang K, Xiang Y, Hsiao H, *et al*. PTEN-induced partial epithelial-mesenchymal transition drives diabetic kidney disease. *J Clin Invest*. 2019;129(3):1129-51.
35. Li K, Yao W, Zheng X, Liao K. Berberine promotes the development of atherosclerosis and foam cell formation by inducing scavenger receptor A expression in macrophage. Cell Res. 2009;19(8):1006-17.
36. Dai XY, Cai Y, Mao DD, Qi YF, Tang C, Xu Q, *et al*. Increased stability of phosphatase and tensin homolog by intermedin leading to scavenger receptor A inhibition of macrophages reduces atherosclerosis in apolipoprotein E-deficient mice. *J Mol Cell Cardiol*. 2012;53(4):509-20.
37. Wang Huizhen JM, Zuo Yangyang, Liang Tiantian, Li Jing, Xie Jianteng, Wang Yanhui, Wen Feng, Zhang Yifan, Li Sheng, Wang Wenjian. Podocyte-specific knock-in of PTEN protects kidney against high fat diet. Chinese Journal of Nephrology. 2018;34(3):192-200.
38. Schmitz G, Grandl M. Role of redox regulation and lipid rafts in macrophages during Ox-LDL-mediated foam cell formation. Antioxid Redox Signal. 2007;9(9):1499-518.
39. Li BH, Yin YW, Liu Y, Pi Y, Guo L, Cao XJ, *et al*. TRPV1 activation impedes foam cell formation by inducing autophagy in oxLDL-treated vascular smooth muscle cells. Cell Death Dis. 2014;5:e1182.
40. Keane WF, Kasiske BL, O'Donnell MP, Kim Y. The role of altered lipid metabolism in the progression of renal disease: experimental evidence. Am J Kidney Dis. 1991;17(5 Suppl 1):38-42.
41. Ricci R, Sumara G, Sumara I, Rozenberg I, Kurrer M, Akhmedov A, *et al*. Requirement of JNK2 for scavenger receptor A-mediated foam cell formation in atherogenesis. Science. 2004;306(5701):1558-61.
42. Osto E, Kouroedov A, Mocharla P, Akhmedov A, Besler C, Rohrer L, *et al*. Inhibition of protein kinase Cbeta prevents foam cell formation by reducing scavenger receptor A expression in human macrophages. Circulation. 2008;118(21):2174-82.
43. Lin CS, Lin FY, Ho LJ, Tsai CS, Cheng SM, Wu WL, *et al*. PKCdelta signalling regulates SR-A and CD36 expression and foam cell formation. Cardiovasc Res. 2012;95(3):346-55.
44. Zuo Yangyang JM, Wang Huizhen, Fu Lei, Wen Feng, Lai Yuxiong, Xie Jianteng, Wang Wenjian. Oxidized LDL leads to podocyte injury through PTEN/SR-A pathway. *Chinese Journal of Nephrology*. 2015;31(10):766-73.
45. Csibi A, Blenis J. Hippo-YAP and mTOR pathways collaborate to regulate organ size. Nat Cell Biol. 2012;14(12):1244-5.
46. Meng Z, Moroishi T, Guan KL. Mechanisms of Hippo pathway regulation. Genes Dev. 2016;30(1):1-17.
47. Campbell KN, Wong JS, Gupta R, Asanuma K, Sudol M, He JC, *et al*. Yes-associated protein (YAP) promotes cell survival by inhibiting proapoptotic dendrin signaling. *J Biol Chem*. 2013;288(24):17057-62.
48. 48.Schwartzman M, Reginensi A, Wong JS, Basgen JM, Meliambro K, Nicholas SB, *et al*. Podocyte-Specific Deletion of Yes-Associated Protein Causes FSGS and Progressive Renal Failure. *J Am Soc Nephrol*. 2016;27(1):216-26.
49. Rinschen MM, Grahammer F, Hoppe AK, Kohli P, Hagmann H, Kretz O, *et al*. YAP-mediated mechanotransduction determines the podocyte's response to damage. Sci Signal. 2017;10(474).
50. Hsueh YJ, Chen HC, Wu SE, Wang TK, Chen JK, Ma DH. Lysophosphatidic acid induces YAP-promoted proliferation of human corneal endothelial cells via PI3K and ROCK pathways. Mol Ther Methods Clin Dev. 2015;2:15014.
51. Fan R, Kim NG, Gumbiner BM. Regulation of Hippo pathway by mitogenic growth factors via phosphoinositide 3-kinase and phosphoinositide-dependent kinase-1. Proc Natl Acad Sci U S A. 2013;110(7):2569-74.
52. Xia H, Dai X, Yu H, Zhou S, Fan Z, Wei G, *et al*. EGFR-PI3K-PDK1 pathway regulates YAP signaling in hepatocellular carcinoma: the mechanism and its implications in targeted therapy. Cell Death Dis. 2018;9(3):269.
53. Maddika S, Kavela S, Rani N, Palicharla VR, Pokorny JL, Sarkaria JN, *et al*. WWP2 is an E3 ubiquitin ligase for PTEN. Nat Cell Biol. 2011;13(6):728-33.
54. Muranen T, Selfors LM, Hwang J, Gallegos LL, Coloff JL, Thoreen CC, *et al*. ERK and p38 MAPK Activities Determine Sensitivity to PI3K/mTOR Inhibition via Regulation of MYC and YAP. Cancer Res. 2016;76(24):7168-80.
55. 55.Wang C, Gu C, Jeong KJ, Zhang D, Guo W, Lu Y, *et al*. YAP/TAZ-Mediated Upregulation of GAB2 Leads to Increased Sensitivity to Growth Factor-Induced Activation of the PI3K Pathway. Cancer Res. 2017;77(7):1637-48.
56. Tumaneng K, Schlegelmilch K, Russell RC, Yimlamai D, Basnet H, Mahadevan N, *et al*. YAP mediates crosstalk between the Hippo and PI(3)K-TOR pathways by suppressing PTEN via miR-29. Nat Cell Biol. 2012;14(12):1322-9.

How to cite this article:

Huizhen Wang M. D *et al* (2019) ' Pten/Yap Mediated Lipid Accumulation in Podocytes Contributes to Glomerulosclerosis', *International Journal of Current Medical and Pharmaceutical Research,* 05(08), pp 4481-4488.

****